Eur. J. Mineral.
2017, **29**, 491–497
Published online 10 January 2017

Hydroxykenoelsmoreite, the first new mineral from the Republic of Burundi

Stuart J. MILLS[1,*], Andrew G. CHRISTY[2,3], Anthony R. KAMPF[4], William D. BIRCH[1] and Anatoly KASATKIN[5]

[1] Geosciences, Museums Victoria, GPO Box 666, Melbourne 3001, Victoria, Australia
*Corresponding author, e-mail: smills@museum.vic.gov.au
[2] Queensland Museum, 122 Gerler Road, Hendra 4011, Queensland, Australia
[3] School of Earth Sciences, University of Queensland, St Lucia 4072, Queensland, Australia
[4] Mineral Sciences Department, Natural History Museum of Los Angeles County, 900 Exposition Blvd., Los Angeles, CA 90007, USA
[5] Fersman Mineralogical Museum of the Russian Academy of Sciences, Leninskiy Prospekt 8-2, 117071 Moscow, Russia

Abstract: We report the new mineral hydroxykenoelsmoreite, which has been approved by the IMA as IMA2016-056. The mineral occurs at the Masaka gold mine, Burundi, as rosettes up to 150 μm across of platy crystals up to 20 μm wide but <2 μm thick, associated with goethite and galena. Crystals are canary yellow, transparent with a vitreous lustre, and have a pale yellow streak. Hydroxykenoelsmoreite is uniaxial (−) and non-pleochroic. The refractive indices were too high to measure, but the Gladstone-Dale compatibility index predicts $n_{ave} = 2.065$. Crystals are brittle with an irregular fracture, but have perfect cleavage on {0 0 1}. The Mohs hardness is ~3 by analogy with hydrokenoelsmoreite. The mineral is a member of the elsmoreite group of the pyrochlore supergroup, but deviates from the ideal cubic symmetry due mainly to ordering of Fe^{3+} onto one of two W sites. Its structure is trigonal, space group $R\bar{3}$, with unit-cell parameters $a = 7.313(2)$, $c = 17.863(7)$ Å, $V = 827(1)$ Å^3 and $Z = 6$. The empirical formula (based on 7 (O + OH) per formula unit (pfu)) is: $(\square_{1.668}Pb_{0.315}Ca_{0.009}\ Na_{0.005}K_{0.003}Ba_{0.001})_{\Sigma 2}(W^{6+}_{1.487}Fe^{3+}_{0.357}Al_{0.156})_{\Sigma 2}(O_{4.119}(OH)_{1.881})_{\Sigma 6}(OH)$. Raman spectroscopy and bond–valence sums showed that molecular H_2O was absent or nearly so. The calculated density is 5.806 g cm^{-3}.

Key-words: Hydroxykenoelsmoreite; pyrochlore; elsmoreite; crystal structure; tungstate.

1. Introduction

Over the past decade, we have been interested in the crystallography and polymorphism of secondary tungstates and antimonates in the pyrochlore group and structures with related hexagonal tungsten bronze (HTB) motifs. We have discovered a number of interesting rhombohedral polytypes which show lowering from the ideal cubic symmetry (*e.g.* hydrokenoelsmoreite-6*R*; Mills *et al.*, 2016a), new pyrochlore-group minerals (*e.g.* hydroxyferroroméite; Mills *et al.*, 2017) and new polysomatic HTB minerals (*e.g.* pittongite; Grey *et al.*, 2006; Birch *et al.*, 2007). As part of this ongoing study, we investigated a sample labelled "phyllotungstite" but with platy morphology similar to pittongite, from the Masaka gold mine, Muyinga Province, Burundi (2°45′56″S, 30°16′38″E). Study of this mineral revealed it to be a new member of the elsmoreite group within the pyrochlore supergroup.

The mineral and name (IMA2016-056) were approved by the IMA–CNMNC prior to publication. The mineral is named according to the nomenclature of the pyrochlore supergroup (Atencio *et al.*, 2010; Christy & Atencio, 2013). Pyrochlore-supergroup minerals have the general stoichiometry $A_2B_2X_6Y$, where the *A* site is 8-coordinated and contains large cations, lone-pair cations or water molecules; the *B* site contains octahedrally 6-coordinated, cations; *X* and *Y* are anion sites; and the $[B_2X_6]$ part of the structure forms a strongly bonded framework of cubic or pseudocubic symmetry, with *A* and *Y* species in structural channels. Species in the supergroup have root-names which depend on the dominant constituents in *B* and *X* sites, with prefixes that are determined by the dominant constituents of dominant valences in *A* and *Y* sites (*cf.* Atencio *et al.*, 2010). The new species described in the present paper is characterized by OH^- dominance at the *Y* site, vacancy at the *A* site and W^{6+} dominance at the *B* site. The type specimen has been lodged in the collections of Museum Victoria, Melbourne, Victoria, Australia, registration number M53606.

2. Occurrence, location and physical and optical properties

The Masaka gold field consists of a 2.5 × 15 km zone of hydrothermal quartz veins hosted in a quartzite and quarztitic conglomerate horizon. There are more than

DOI: 10.1127/ejm/2017/0029-2618
0935-1221/17/0029-2618 $ 3.15

40 workings in the zone which have been artisanally mined. The Masaka gold mine itself is a resource of ~130,500 oz (4200 g) at 1.01 g t^{-1} Au (Potvin, 2012).

Hydroxykenoelsmoreite forms minute platy canary-yellow crystals up to about 50 μm across. Generally, crystals are <20 μm across and extremely thin (~2 μm). The platy crystals are intergrown to form loose rosettes up to about 150 μm across (Fig. 1). The dominant form is {0 0 1}; no bounding forms could be measured, but based upon the appearance of rare hexagonal tablets, the form {0 0 1} occurs, with either {1 0 0} or {1 1 0}. Crystals are transparent with a vitreous lustre, are brittle with an irregular fracture and have perfect cleavage on {0 0 1}. The streak is pale yellow. The Mohs hardness is ~3 by analogy with hydrokenoelsmoreite (Williams *et al.*, 2005). The density could not be measured because it exceeds that of available liquids, however the density calculated for the empirical formula $(\square_{1.668}Pb_{0.315}Ca_{0.009}Na_{0.005}K_{0.003}Ba_{0.001})_{\Sigma 2}(W_{1.487}Fe_{0.357}Al_{0.156})_{\Sigma 2}(O_{4.119}(OH)_{1.881})_{\Sigma 6}(OH)$ is 5.806 g cm^{-3}.

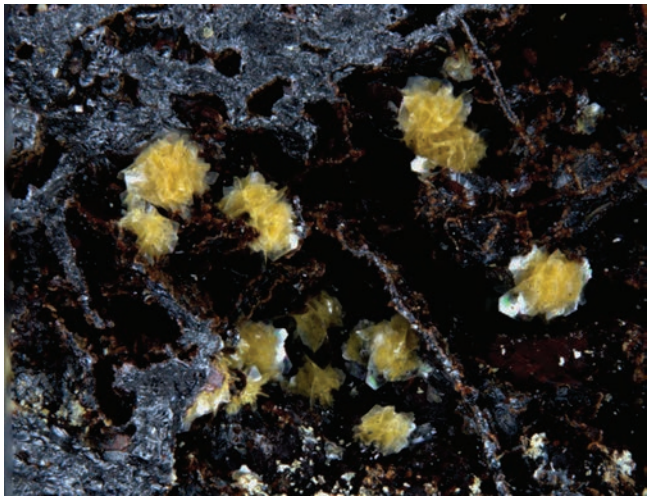

Fig. 1. Clusters of hydroxykenoelsmoreite on goethite. Field of view approximately 0.8 mm. (Online version in colour.)

Hydroxykenoelsmoreite is uniaxial (−) and non-pleochroic. The indices of refraction could not be measured because of the small amount of material available and the difficulty in working with liquids of sufficiently high index of refraction. The Gladstone–Dale compatibility index predicts $n_{ave} = 2.065$.

The type specimen of hydroxykenoelsmoreite measures only 0.5 × 0.5 cm, and to the best of our knowledge is the only specimen in existence. The only other species associated on the type specimen are goethite and galena.

3. Spectroscopy

Raman spectra were recorded using a Renishaw RM 2000 confocal micro-Raman System equipped with a near-IR diode laser at a wavelength of 782 nm (laser power = 1.15 mW and laser spot size = 1 μm). The Raman spectrum was collected by fine-focusing a 50× microscope objective and the data acquisition time was 10 s.

The Raman spectrum (Fig. 2) is characterized by a very intense band at 929 cm^{-1} (W = O stretching). Weak bands at 853 and 691 cm^{-1} and 476 and 402 cm^{-1} correspond to O–W–O stretching and O–W–O bending modes, respectively (Gu *et al.*, 2006). Bands in the region 100–350 cm^{-1} correspond to lattice modes. Two broad bands at 2923 and 3443 cm^{-1} are assigned to O–H stretching modes, although we note that these stretching frequencies are low for an OH group that is essentially not hydrogen-bonded: according to the structure refinement (below), the next nearest oxygen atoms to O2 are 3 × O3 at 2.96 Å and 3 × O1 at 3.17 Å. There is at best only a very weak indication of H–O–H bending modes at 1610 cm^{-1}, consistent with H_2O being almost absent in the *Y* site. Although lack of the 1600 cm^{-1} band is not always reliable as an indicator of absent molecular H_2O,

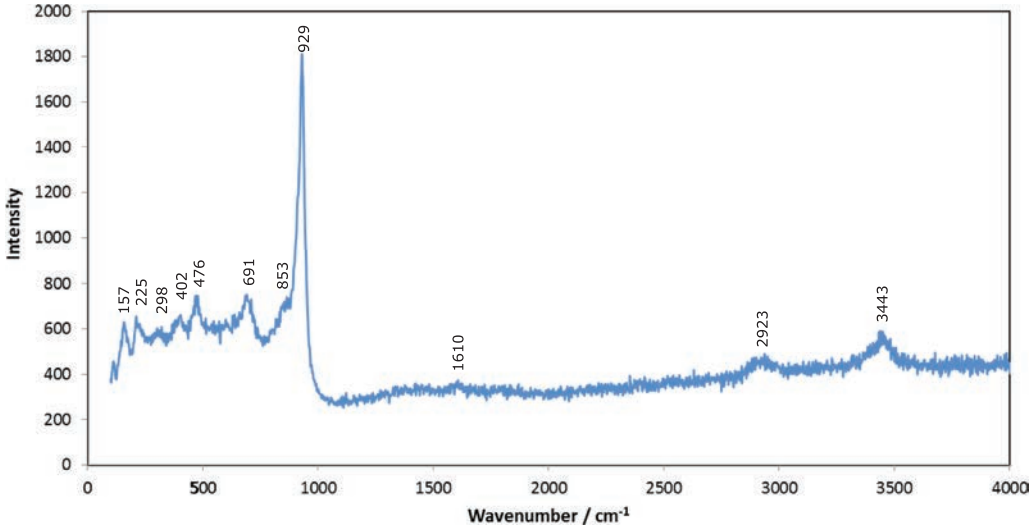

Fig. 2. Raman spectrum of hydroxykenoelsmoreite collected in the 100–4000 cm^{-1} region. (Online version in colour.)

occupation of the *Y* site (O2) by OH^- instead is also consistent with the bond valence sum derived from the structure refinement below.

4. Chemical composition

Four quantitative chemical analyses were carried out by means of an electron microprobe (wavelength-dispersive spectrometry mode (WDS), 15 kV, 20 nA and 5 μm beam diameter) at The University of Melbourne. The structure refinement (see below) gave a very low scattering factor for the W1 site, implying significant substitution of a lighter element, so Fe was assumed to be Fe^{3+} in the *B* site. Since the refinement indicated full occupancy of the *Y* site, the number of oxygen atoms in the anhydrous formula was calculated, and H_2O then calculated on the basis of 7 (O + OH) pfu. Since the Raman spectrum showed no significant H_2O bending modes (see above), O^{2-} and H_2O in first *Y* and then *X* sites were combined to form 2 OH^- as far as possible. No other elements were detected. Analytical data are given in Table 1.

The empirical formula (based on 7 (O + OH) pfu) is: $(\square_{1.668}Pb_{0.315}Ca_{0.009}Na_{0.005}K_{0.003}Ba_{0.001})_{\Sigma 2}(W_{1.487}Fe_{0.357}Al_{0.156})_{\Sigma 2}(O_{4.119}(OH)_{1.881})_{\Sigma 6}(OH)$. The name corresponds to predominance of vacancies in the *A* site, W in *B* and OH^- in *Y*. The end-member composition which corresponds most directly to these conditions would be $\square_2W_2O_6(OH)$, except that this formula is not electrically neutral, and physically realizable compositions must always have heterovalent substituents in one or more sites; the type material has substantial substitutions in *A*, *B* and *X* sites. If the 0.325 A^{2+} cations, 0.008 A^{1+} cations and 0.513 B^{3+} cations are represented by their respective dominant examples, Pb^{2+}, Na^+ and Fe^{3+}, the formula simplifies to $(\square_{1.668}Pb_{0.325}Na_{0.008})_{\Sigma 2}(W_{1.487}Fe_{0.513})_{\Sigma 2}(O_{4.119}(OH)_{1.881})_{\Sigma 6}(OH)$. From this formula, it is possible to extract charge-balanced end-members in the sense of Hawthorne (2002) at the following maximum percentages:

- End-member A, $\square_2W_2(O_5(OH))_{\Sigma 6}(OH)$: 74.3% (limited by ^{B}W)
- End-member B, $(\square_{1.5}Pb_{0.5})_{\Sigma 2}W_2O_6(OH)$: 65.0% (limited by ^{A}Pb)
- End-member C, $(\square_{1.5}Pb_{0.5})_{\Sigma 2}Fe_2(OH)_6(OH)$: 25.7% (limited by ^{B}Fe)
- End-member D, $Pb_2Fe_2(O_3(OH)_3)_{\Sigma 6}(OH)$: 16.3% (limited by ^{A}Pb)
- End-member E, $Pb_2(WFe)_{\Sigma 2}O_6(OH)$: 16.3% (limited by ^{A}Pb)
- End-member F, $(\square Na)_{\Sigma 2}W_2O_6(OH)$: 0.8% (limited by ^{A}Na)

These maximum percentages are obtained only if the corresponding end-member is the first to be extracted from the original charge-arrangement formula $(\square_{1.667}Pb_{0.325}Na_{0.008})_{\Sigma 2}(W_{1.487}Fe_{0.513})_{\Sigma 2}(O_{4.119}(OH)_{1.881})_{\Sigma 6}(OH)$. There is no implication that successive end-members are to be extracted sequentially. Indeed, if that procedure is followed, then: (i) the percentages of later end-members can be reduced below the absolute maximum, because necessary components have already been extracted; and (ii) the numbers obtained are not reproducible, in that they depend on the order in which end-members are extracted, as shown in Atencio *et al.* (2010).

Table 1. Analytical data (wt%) for hydroxykenoelsmoreite. Water content calculated from charge balance and structure refinement.

Constit.	Mean	Range	SD	Probe standard
Na_2O	0.03	0–0.05	0.02	Jadeite
K_2O	0.03	0–0.02	0.01	$KTaO_3$
CaO	0.10	0.03–0.18	0.07	Wollastonite
BaO	0.03	0–0.04	0.02	Baryte
PbO	14.77	14.42–15.71	0.63	Pb metal
Al_2O_3	1.67	1.26–1.86	0.28	Al_2O_3
Fe_2O_3	5.99	5.37–7.13	0. 78	Hematite
WO_3	72.39	71.62–73.18	0.64	W metal
H_2O_{calc}	5.45			
Total	100.46			

Note that formulae A–E share a common two-dimensional composition space, although F does not because of its Na/K content. The charge arrangement above can be projected into the A–E plane if $Na_{0.008}$ is replaced by $(\square_{0.004}Pb_{0.004})$ to give $(\square_{1.671}Pb_{0.329})_{\Sigma 2}(W_{1.487}Fe_{0.513})_{\Sigma 2}(O_{4.119}(OH)_{1.881})_{\Sigma 6}(OH)$. This overall charge arrangement can then be captured in terms of the three dominant end-members as 40.1% B, 34.2% A and 25.7% C (Fig. 3). Note that B is dominant when the formula is decomposed in this way. The mineral composition highlights the complexities associated with charge-coupled substitutions involving sites of different multiplicities and elements of a wide range of valences.

- The large number of charge arrangements that make substantial contributions to the overall composition illustrates why for the pyrochlore supergroup it would be unwieldy to apply the maximum-percentage end-member approach used to define and identify garnet species by Grew *et al.* (2013).
- Both of the predominant end-members A and B correspond to the name "hydroxykenoelsmoreite", according to the pyrochlore-supergroup nomenclature rules of Atencio *et al.* (2010) (Fig. 3). Thus, there is not a unique end-member whose composition can be used as an ideal formula for this mineral, although end-member A is dominant in this case.

5. X-ray diffraction and crystallography

X-ray powder diffraction data were obtained using a Rigaku R-Axis Rapid II curved imaging plate micro-diffractometer utilizing monochromatised Mo*K*α radiation. Observed powder *d*-values and intensities were derived by profile fitting using JADE 2010 software. Data are given in Table 2. The unit cell ($R\bar{3}$, $a = 7.313(2)$, $c = 17.863(7)$ Å, $V = 827(1)$ Å^3 and $Z = 6$) is in good agreement with the single-crystal data below.

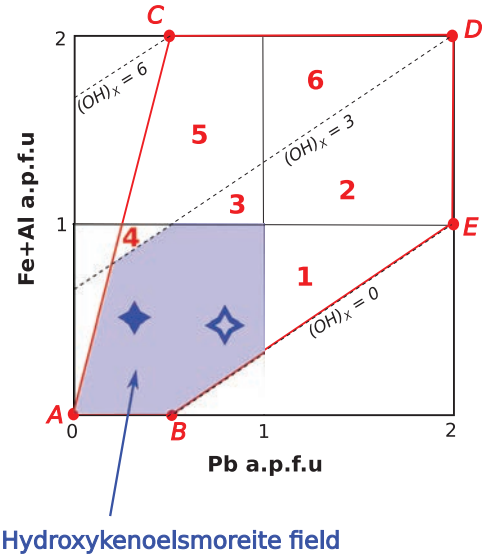

Fig. 3. Two-dimensional composition space assuming that *Y* site is fully occupied by OH^-, showing end-members A–E (red filled circles), possible pyrochlore-supergroup compositions (red polygon), composition of the new mineral (blue stars: filled = WDS, open = structure refinement) and subfield corresponding to the name "hydroxykenoelsmoreite" (blue polygon). Composition fields for additional potential new species are numbered 1–6 in red: 1 = "hydroxyplumboelsmoreite", 2 = "hydroxyplumborootname1", 3 = "hydroxykenorootname1", 4 = "hydroxyplumborootname2", 5 = "hydroxykenorootname3", 5 = "hydroxyplumborootname3": "Rootname1" has Fe dominant in *B* sites, O in *X* sites; "rootname2" has W dominant in *B* sites, OH in *X* sites; "rootname3" has Fe dominant in *B* sites and OH in *X* sites. (Online version in colour.)

Single-crystal data were collected at 100(2) K using an ADSC Quantum 315r detector and monochromatic radiation with a wavelength of 0.71073 Å at the Australian Synchrotron. A ϕ scan was employed, with frame widths of 1° and a counting time per frame of 1 s. The data were integrated in *P*1 using XDS (Kabsch, 2010); XPREP (Bruker, 2001) gave a space group of $R\bar{3}$. The absorption correction was carried out with SADABS (Bruker, 2001), giving 1299 reflections with an R_{int} of 0.1958. The large R_{int} is due to streaking observed along **c***, as well as the poorly diffracting nature of the thin platelet. The structure of hydroxykenoelsmoreite was solved in space group $R\bar{3}$ (No. 148) by direct methods using SHELXS-97 and subsequent difference Fourier syntheses followed by full-matrix least-squares refinement on F^2 using SHELXL-97 (Sheldrick, 2008). The initial position of the heavy Pb and W ions were easily located. The O atoms were then located by subsequent inspection of the difference Fourier maps. Following placement of the atoms and anisotropic treatment of the Pb and W atoms, the occupancy of the O1 atom and refinement of electron count at the W sites were performed. The O1 site was shown to be split, and the refined occupancy of O1 of 83% was fixed and O1a then fixed to 17%, with the U_{eq} of O1 and O1a constrained to be equal at 0.01 $Å^2$. The W:Fe ratio was also fixed after refinement. Data collection details are provided in Table 3, atom fractional coordinates and displacement parameters in Table 4, bond lengths in Table 5 and bond–valence sums in Table 6.

Table 2. X-ray powder diffraction data (*d* in Å) for hydroxykenoelsmoreite.

I_{obs}	d_{obs}	d_{calc}	I_{calc}	*h k l*
51	5.99	5.9490	37	1 0 1
64	3.128	3.1071	22	1 1 $\bar{3}$
100	2.983	2.9745	100	2 0 2
32	2.582	2.5764	34	0 2 4
6	2.383	2.3651	1	1 0 7
		2.3638	2	2 1 1
		2.1035	1	1 2 $\bar{4}$
10	1.9880	1.9842	2	0 0 9
		1.9830	4	3 0 3
57	1.8249	1.8222	18	2 0 8
		1.8214	20	2 2 0
12	1.7451	1.7425	4	1 1 $\bar{9}$
		1.7417	3	2 2 3
12	1.5811	1.5722	1	0 1 11
		1.5714	2	3 1 5
47	1.5579	1.5536	37	2 2 $\bar{6}$
14	1.4901	1.4882	3	0 0 12
		1.4873	7	4 0 4
10	1.4480	1.4433	3	3 0 9
		1.4428	1	3 2 1
7	1.3425	1.3420	2	1 2 11
		1.3414	2	1 4 3
6	1.2905	1.2882	4	0 4 8
20	1.1863		1	3 1 11
		1.1902	1	3 3 $\bar{3}$
		1.1898	3	2 0 14
		1.1826	2	4 0 10
		1.1822		
		1.1819		
5	2 4 $\bar{2}$			
13	1.1541	1.1524	5	2 2 12
		1.1520	4	2 4 4
5	1.1353	1.1312	2	1 4 9

Hydroxykenoelsmoreite is isotypic with members of the pyrochlore supergroup (Atencio *et al.*, 2010), which has the ideal pyrochlore stoichiometry $A_2B_2X_6Y$. As described in Mills *et al.* (2016a) and Atencio (2016), a number of different non-cubic pyrochlore polytypes exist; the most common of these is 3*R* with the space group $R\bar{3}m$. Descent in symmetry splits the *A*, *B* and *X* sites such that the structure is crystallographically $(A1)_3(A2)_1(B1)_3(B2)_1(X_1)_6(X2)_6Y_2$. The hydroxykenoelsmoreite studied here is the 3*R* polytype but, unlike hydrokenomicrolite-3*R* (Atencio, 2016), the symmetry is further lowered to $R\bar{3}$, due to very small rotations of coordination polyhedra that are not associated with further site splitting. In the structure refinement below,

the *A*1, *A*2, *B*1, *B*2, *X*1, *X*2 and *Y* sites are respectively labelled Pb2, Pb1, W1, W2, O1, O3 and O2. The structure is shown in Fig. 4.

In hydroxykenoelsmoreite, both *A* sites are partially occupied by Pb, with occupancies of 0.34(3) and 0.41(3), respectively for Pb1 and Pb2 (Table 4). Ordering in the *B* sites is also observed, where W2 is fully occupied by W, while the low scattering factor for W1 implies that Fe + Al substitute for W. The site scattering factor for W1 corresponds to $W_{0.78}Fe_{0.22}$. Thus, the refined structure corresponds to a charge-balanced formula $(\square_{1.215}Pb_{0.785})_{\Sigma 2}(W_{1.56}Fe_{0.44})_{\Sigma 2}(O_{5.25}(OH)_{0.75})_{\Sigma 6}(OH)$, which while still in the hydroxykenoelsmoreite field of Fig. 3, has more than twice the Pb content of the microprobe analysis. This implies that the Pb content is variable between crystals, and probably between zones within crystals, and that there is substantial solid solution towards "hydroxyplumboelsmoreite". Minerals of the pyrochlore supergroup show extensive solid solution behaviour, and complex zonation appears to be common (*cf*. Brugger *et al.*, 1997; Christy & Gatedal, 2005; Mills *et al.*, 2016b).

Table 3. Data collection and structure refinement details for hydroxykenoelsmoreite.

Diffractometer	ADSC Quantum 315r detector
X-ray radiation	Synchrotron
Temperature	100(2) K
Space group	$R\overline{3}$
Unit-cell dimensions	$a = 7.2855(10)$ Å
	$c = 17.858(4)$
V	820.9(2) Å^3
Z	6
Absorption coefficient	27.130 mm^{-1}
$F(0\,0\,0)$	723
θ range	3.42 to 23.25°
Index ranges	$-7 \le h \le 8$, $-8 \le k \le 8$, $-19 \le l \le 19$
Reflections collected/unique	1299/265 [$R_{int} = 0.1958$]
Reflections with $F_o > 4\sigma(F)$	198
Refinement method	Full-matrix least-squares on F^2
Parameters refined/restraints	32/0
Final R indices [$F_o > 4\sigma(F)$]	$R_1 = 0.1388$, w$R_2 = 0.1500$
R indices (all data)	$R_1 = 0.3366$, w$R_2 = 0.3523$
Extinction coefficient	0.017(6)
GoF	1.417

Bond distances for *A* and *B* cations are shown in Table 5. These have been used to calculate the bond valences and bond–valence sums of Table 6. The bond–valence sums are significantly different for the two types of *B* site: only 4.96 *v.u.* for W1, but 6.33 *v.u.* for W2, consistent with trivalent cations being ordered completely at W1. The WDS analyses (above) imply higher (Fe + Al) content and hence even lower BVS for W1. Preferential ordering of the trivalent cations into W1 is thus the main reason for departure from cubic symmetry in hydroxykenoelsmoreite-3*R*. Bond valence sums show that O2 is OH and O3 is O, with BVS sums of 0.96 and 2.09 *v.u.*, respectively (Table 5). O1 is split into two mutually exclusive sites that are 0.63 Å apart, with O1 (83% occupied) having a BVS of 1.93 *v.u.*, while O1a (17%) has a BVS of 1.41 *v.u*, suggesting that the reason for this additional splitting is concentration of ^{X}(OH) into O1a. O1 is bound strongly (0.87 *v.u.*) to 2 × W1 and more weakly (~0.25 *v.u.*) to Pb1 and Pb2, while O1a is bound strongly to Pb1 (0.79 *v.u.*), and moderately strongly to 2 × W1 (~0.54 *v.u.*), but only weakly to Pb2 (0.13 *v.u.*). Partitioning of OH into O1 and the associated splitting is reasonable, since this is the *X* site that links two W1 octahedra, where the low-valence *B* cations are situated. However, 17% occupancy of the O1a site corresponds to about 1 *X* atom pfu. The mineral of the present study may have 1.88 ^{X}OH$^-$ pfu (WDS) or 0.75 ^{X}OH$^-$ (structure), suggesting that there must be respectively either some OH$^-$ at O1 as well (leading to BVS < 2 *v.u.*), or some O^{2-} at O1a (hence BVS > 1 *v.u.*). Thus, the occupancies and BVS patterns correlate well with both the Raman and electron–microprobe analyses.

6. Conclusion

We report a member of the pyrochlore supergroup which is the first new mineral to be reported from the Republic of Burundi. The mineral has largely vacant *A* sites, W^{6+} preponderant in *B* sites and OH$^-$ in the *Y* site, and hence is named hydroxykenoelsmoreite in accord with the nomenclature scheme of Atencio *et al.* (2010). Pb^{2+} in the *A* sites demonstrates solid solution towards a hypothetical "plumboelsmoreite" species. Note that a mineral of that compositional type was described and

Table 4. Atom coordinates and displacement parameters (Å^2) for hydroxykenoelsmoreite.

	Wyckoff site	x	y	z	U_{eq}	Occ.	U^{11}	U^{22}	U^{33}	U^{23}	U^{13}	U^{12}
Pb1	3*a*	0	0	0	0.046(9)	0.34(3)	0.031(11)	0.031(11)	0.074(16)	0	0	0.016(5)
Pb2	9*d*	1/6	1/3	5/6	0.062(9)	0.41(3)	0.054(12)	0.070(14)	0.069(13)	−0.013(3)	−0.005(3)	0.036(7)
W1	9*e*	1/2	1/2	0	0.030(3)	0.78	0.023(4)	0.024(4)	0.044(4)	−0.0018(9)	0.0016(9)	0.013(2)
Fe1	9*e*	1/2	1/2	0	0.030(3)	0.22	0.023(4)	0.024(4)	0.044(4)	−0.0018(9)	0.0016(9)	0.013(2)
W2	3*b*	2/3	1/3	5/6	0.042(3)	1	0.041(4)	0.041(4)	0.045(5)	0	0	0.020(2)
O1	18*f*	0.797(3)	0.203(3)	0.0182(13)	0.01	0.83						
O1a	18*f*	0.834(15)	0.163(14)	0.000(7)	0.01	0.17						
O2	6*c*	1/3	2/3	0.812(3)	0.081(18)	1						
O3	18*f*	0.550(3)	0.455(3)	0.8961(12)	0.022(6)	1						

approved as jixianite (Liu, 1979), but by modern criteria remains inadequately characterized for the exact species name to be ascertained. Hence, jixianite is currently of 'questionable' status (Christy & Atencio, 2013). Although dominant end-member criteria are not used to assign species names in the pyrochlore supergroup, the end-member $\square_2W_2(O_5(OH))_{\Sigma 6}(OH)$ comprises >74% of the mineral of the present study. The new mineral joins a growing list of pyrochlore-supergroup species in which the symmetry is lowered due to ordering on either *A* sites or *B* sites (*cf.* Ercit *et al.*, 1986; Rouse *et al.*, 1998; Andrade *et al.*, 2017; Atencio, 2016; Mills *et al.*, 2016a).

Table 5. Selected bond distances (Å) for hydroxykenoelsmoreite. Note that O1 and O1a occur as mutually exclusive pairs, occupied in an 83:17 ratio.

Atom	Distance	Multiplicity
Pb1		
O1a	2.08(10)	6
O1	2.58(2)	6
O2	2.60(6)	2
Mean	2.52(17)	
Pb2		
O2	2.136(11)	2
O1	2.69(2)	2
O1a	2.98(6)	2
O3	2.691(14)	2
O3	2.714(14)	2
Mean	2.53(28)	
W1		
O1	1.94(2)	2
O1	1.94(2)	2
O1a	2.10(9)	2
O1a	2.13(9)	2
O3	1.95(2)	2
Mean	1.96(6)	
W2		
O3	1.874(18)	6

Acknowledgements: Simon Hinkley is thanked for help with taking the image of the type specimen. E.V. Galuskin and A.S. Zolotarev are thanked for their comments, which helped improve the manuscript.

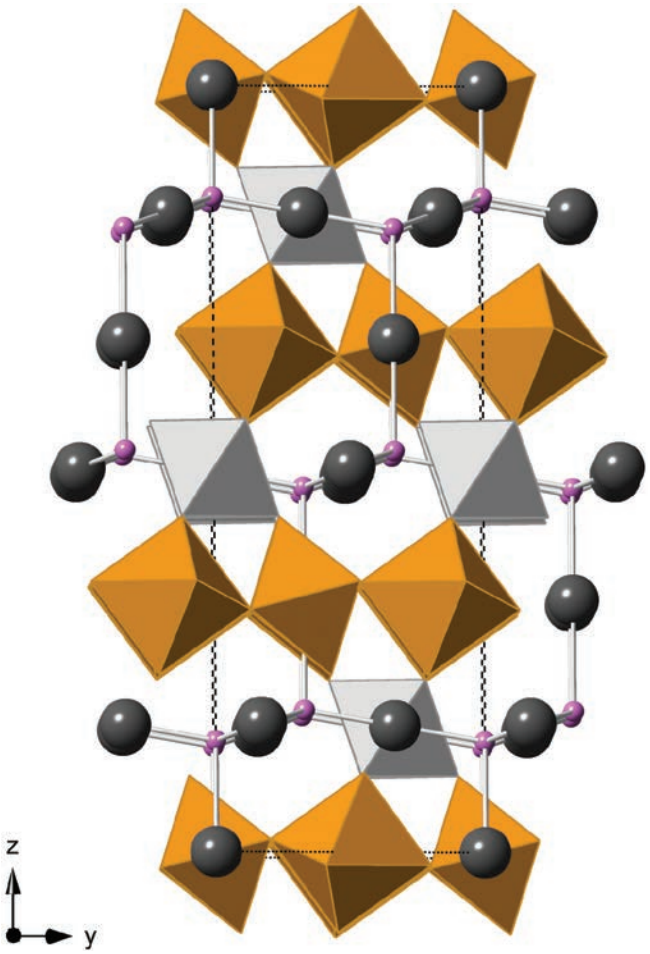

Fig. 4. Crystal structure of hydroxykenoelsmoreite, viewed along *a*. Brown octahedra are W1, containing some (Fe^{3+} + Al), light grey octahedra are W2, and dark grey spheres are partially occupied Pb sites, connected into a network through non-framework OH^- anions O2 (pink spheres). (Online version in colour.)

Table 6. Bond–valence sums for hydroxykenoelsmoreite, taking into account partial occupancy of Pb1, Pb2, O1, O1a and 78:22 ratio of W:Fe in W1 site. Bond–valence parameters are those of Brese & O'Keeffe (1991); except for Pb–O from Krivovichev & Brown (2001).

	Pb1	Pb2		W1		W2	Sum
O1	0.283 ×4.98 ↓, ×0.34 →	0.227 ×1.66 ↓, ×0.41 →		0.869 ×1.66 ↓	0.853 ×1.66 ↓		1.927
O1a	0.794 ×1.02 ↓, ×0.34 →	0.126 ×0.34 ↓, ×0. 41 →		0.556 ×0.34 ↓	0.548 ×0.34 ↓		1.408
O2	0.275 ×2 ↓, ×0.34→	0.701 ×2 ↓, ×1.23→					0.956
O3		0.227 ×2 ↓, ×0. 41 →	0.216 ×2 ↓, ×0. 41 →	0.852 ×2 ↓		1.055 ×6 ↓	2.089
Sum	2.769	2.708		4.959		6.331	

References

Andrade, M.B., Yang, H., Atencio, D., Downs, R.T., Chukanov, N. V., Lemée-Cailleau, M.H., Persiano, A.I.C., Goeta, A.E., Ellena, J. (2017): Hydroxycalciomicrolite, $Ca_{1.5}Ta_2O_6(OH)$, a new member of the microlite group from Volta Grande pegmatite, Nazareno, Minas Gerais, Brazil. *Mineral. Mag.*, **81**, doi: 10.1180/minmag.2016.080.116.

Atencio, D. (2016): Parabariomicrolite discredited as identical to hydrokenomicrolite-3*R*. *Mineral. Mag.*, **80**, 923–924.

Atencio, D., Andrade, M.B., Christy, A.G., Gieré, R., Kartashov, P. M. (2010): The pyrochlore supergroup of minerals: nomenclature. *Can. Mineral.*, **48**, 673–698.

Brese, N.E. & O'Keeffe, M. (1991): Bond-valence parameters for solids. *Acta Crystallogr.*, **B47**, 192–197.

Birch, W.D., Grey, I.E., Mills, S.J., Bougerol, C., Pring, A., Ansermet, S. (2007): Pittongite: a new secondary mineral from Pittong, Victoria, Australia. *Can. Mineral.*, **45**, 857–864.

Brugger, J., Gieré, R., Graeser, S., Meisser, N. (1997): The crystal chemistry of roméite. *Contrib. Mineral. Petrol.*, **127**, 136–146.

Bruker (2001): SADABS and XPREP. Bruker AXS Inc., Madison, Wisconsin, USA.

Christy, A.G. & Atencio, D. (2013): Clarification of status of species in the pyrochlore supergroup. *Mineral. Mag.*, **77**, 13–20.

Christy, A.G. & Gatedal, K. (2005): Extremely Pb-rich rock-forming silicates including a beryllium scapolite and associated minerals in a skarn from Långban, Värmland, Sweden. *Mineral. Mag.*, **69**, 995–1018.

Ercit, T.S., Hawthorne, F.C., Černý, P. (1986): Parabariomicrolite, a new species and its structural relationship to the pyrochlore group. *Can. Mineral.*, **24**, 655–663.

Grew, E.S., Locock, A.J., Mills, S.J., Galuskina, I.O., Galuskin, E. V., Hålenius, U. (2013): Nomenclature of the garnet supergroup. *Am. Mineral.*, **98**, 785–810.

Grey, I.E., Birch, W.D., Bougerol, C., Mills, S. J. (2006): Unit-cell intergrowth of pyrochlore and hexagonal tungsten bronze structures in secondary tungsten minerals. *J. Solid State Chem.*, **179**, 3860–3869.

Gu, Z., Ma, Y., Zhai, T., Gao, B., Yang, W., Yao, J. (2006): A simple hydrothermal method for the large-scale synthesis of single-crystal potassium tungsten bronze nanowires. *Chem. Eur. J.*, **12**, 7717–7723.

Hawthorne, F.C. (2002): The use of end-member charge-arrangements in defining new mineral species and heterovalent substitutions in complex minerals. *Can. Mineral.*, **40**, 699–710.

Kabsch, W. (2010): XDS. *Acta Crystallogr.*, **D66**, 125–132.

Krivovichev, S.V. & Brown, I.D. (2001): Are the compressive effects of encapsulation an artifact of the bond valence parameters? *Z. Kristallogr.*, **216**, 245–247.

Liu, J. (1979): Jixianite $Pb(W, Fe^{3+})_2(O, OH)_7$–a new tungsten mineral. *Acta Geol. Sin.*, **53**, 45–49. (in Chinese with English abs.)

Mills, S.J., Christy, A.G., Rumsey, M.S., Spratt, J.G. (2016a): The crystal chemistry of elsmoreite from the Hemerdon (Drakelands) mine, UK: hydrokenoelsmoreite-3*C* and hydrokenoelsmoreite-6*R*. *Mineral. Mag.*, **80**, 1195–1203.

Mills, S.J., Christy, A.G., Rumsey, M.S., Spratt, J. (2016b): Discreditation of partzite. *Eur. J. Mineral.*, **28**, 1019–1024.

Mills, S.J., Christy, A.G., Rumsey, M.S., Spratt, J., Bittarello, E., Favreau, G., Ciriotti, M.E., Berbain, C. (2017): Hydroxyferroroméite, a new secondary mineral from Oms, France. *Eur. J. Mineral.*, **29**, 307–314.

Potvin, J.C. (2012): Flemish gold corp. London December 2012 update, 31 p.

Rouse, R.C., Dunn, P.J., Peacor, D.R., Wang, L. (1998): Structural studies of the natural antimonian pyrochlores I. Mixed valency, cation site splitting, and symmetry reduction in lewisite. *J. Solid State Chem.*, **141**, 562–569.

Sheldrick, G.M. (2008): A short history of *SHELX*. *Acta Crystallogr.*, **A64**, 112–122.

Williams, P.A., Leverett, P., Sharpe, J.L., Colchester, D.M. (2005): Elsmoreite, cubic $WO_3{\cdot}0.5H_2O$, a new mineral species from Elsmore, New South Wales. *Can. Mineral.*, **43**, 1061–1064.

Received 18 October 2016
Modified version received 15 November 2016
Accepted 30 November 2016